

Experimental demonstration of silicon nitride waveguide gratings with excellent efficiency and divergence angle

Zhaozhen Chen(陈兆震), Wenling Li(李文玲), Qian Wang(王乾), Enfeng Liu(刘恩峰), Xinqun Zhang(张新群), Jingwei Liu(刘敬伟), and Zhengsheng Han(韩郑生)

Citation: Chin. Phys. B, 2025, 34 (**5**): 054206. DOI: 10.1088/1674-1056/adbbbf
http://cpb.iphy.ac.cn; http://iopscience.iop.org/cpb

What follows is a list of articles you may be interested in

Silicon-based optoelectronic heterogeneous integration for optical interconnection

Le-Liang Li(李乐良), Gui-Ke Li(李贵柯), Zhao Zhang(张钊), Jian Liu(刘剑), Nan-Jian Wu(吴南健), Kai-You Wang(王开友), Nan Qi(祁楠), and Li-Yuan Liu(刘力源)
Chin. Phys. B, 2024, 33 (**2**): 024201. DOI: 10.1088/1674-1056/ad0e5b

Compact TE-pass polarizer based on lithium-niobate-on-insulator assisted by indium tin oxide and silicon nitride

Jia-Min Liu(刘家敏) and De-Long Zhang(张德龙)
Chin. Phys. B, 2023, 32 (**6**): 064208. DOI: 10.1088/1674-1056/ac960b

High-performance and fabrication friendly polarization demultiplexer

Huan Guan(关欢), Yang Liu(刘阳), and Zhiyong Li (李智勇)
Chin. Phys. B, 2022, 31 (**3**): 034203. DOI: 10.1088/1674-1056/ac21bc

Bandwidth-tunable silicon nitride microring resonators

Jiacheng Liu(刘嘉成), Chao Wu(吴超), Gongyu Xia(夏功榆), Qilin Zheng(郑骑林), Zhihong Zhu(朱志宏), and Ping Xu(徐平)
Chin. Phys. B, 2022, 31 (**1**): 014201. DOI: 10.1088/1674-1056/ac2e64

Low-power electro-optic phase modulator based on multilayer graphene/silicon nitride waveguide

Lanting Ji(姬兰婷), Wei Chen(陈威), Yang Gao(高阳), Yan Xu(许言), Chi Wu(吴锜), Xibin Wang(王希斌), Yunji Yi(衣云骥), Baohua Li(李宝华), Xiaoqiang Sun(孙小强), Daming Zhang(张大明)
Chin. Phys. B, 2020, 29 (**8**): 084207. DOI: 10.1088/1674-1056/ab943b

---

Experimental demonstration of silicon nitride waveguide gratings with excellent efficiency and divergence angle

Zhaozhen Chen(陈兆震)[1,2], Wenling Li(李文玲)[3], Qian Wang(王乾)[4], Enfeng Liu(刘恩峰)[4], Xinqun Zhang(张新群)[3], Jingwei Liu(刘敬伟)[3,†], and Zhengsheng Han(韩郑生)[1,2,‡]

[1] *Institute of Microelectronics of the Chinese Academy of Sciences, Beijing* 100029, *China*
[2] *University of Chinese Academy of Sciences, Beijing* 100049, *China*
[3] *China Science Photon Chip (Haining) Technology Co., Ltd., Haining* 314499, *China*
[4] *Beijing YanDong MicroElectronic Technology Co., Ltd., Beijing* 100006, *China*

(Received 11 November 2024; revised manuscript received 6 January 2025; accepted manuscript online 3 March 2025)

Silicon nitride (Si_3N_4) photonic platform has recently attracted increasing attention for Si_3N_4 photonic integrated circuits (PIC). A diffraction grating with the only etched top-layer in tri-layer Si_3N_4 optical waveguides is proposed, which shows a simple fabrication process, high upward diffraction efficiency, and lower far-field divergence angle. The measured results of the diffraction grating at a wavelength of 905 nm show the average upward diffraction efficiency of 90.5% and average far-field divergence angle of 0.154°, which shows a good agreement with the design results with the upward diffraction efficiency of 91.6% and far-field divergence angle of 0.105°.

Keywords: silicon nitride, photonic platform, optical waveguides

PACS: 42.79.–e, 42.82.–m

DOI: 10.1088/1674-1056/adbbbf **CSTR:** 32038.14.CPB.adbbbf

1. Introduction

Silicon nitride photonic platform has recently attracted increasing attention,[1–4] which is transparent in both visible and infrared spectra,[4,5] and can be readily prepared by conventional deposition technologies.[4,6] Moreover, the moderate index contrast can reduce the scattering loss due to the sidewall roughness, and allow a high fabrication tolerance.[7,8] However, Si_3N_4 waveguide grating couplers have a lower coupling efficiency due to a lower index contrast.[7,9,10] Some methods are proposed to improve the coupling efficiency. For example, bottom reflectors such as a metal mirror[11,12] and distributed Bragg reflector[8,9,13] have been used to improve the coupling efficiency, since a majority of the optical power is reflected downward into the substrate. However, this increase the process complexity or be incompatible with the subsequent high-temperature processes.[14]

Hence, an offset single or double layer Si_3N_4 waveguide grating structure does not require a reflector and is theoretically proven to have an upward diffraction efficiency above 90% at a wavelength of 1550 nm.[15,16] However, this structure still requires two steps of lithography and an accurate overlay between masks, which is a complicated preparation process. A multi-layer Si_3N_4 waveguide diffraction gratings with a upward efficiency of above 90% is theoretically demonstrated at a wavelength of 850 nm, which need only one lithography step on the diffractive region due to no additional reflective layer.[14] Moreover, the multi-layer Si_3N_4 waveguide shows a low propagation loss and high design flexibility.[17]

In this paper, a top-layer etching diffraction grating in tri-layer Si_3N_4 waveguides is designed. A preparation process is introduced to fabricate the waveguide diffraction grating coupler. Four testing sample of the diffraction grating are fabricated, which consists of a diffraction grating for light output from waveguides, a coupling grating for light input into waveguide, and a waveguide beam expander. The fabricated top-layer etching diffraction grating in tri-layer Si_3N_4 waveguide is measured, the losses, upward diffraction efficiency, and far-field divergence angle are evaluated for the top-layer etching diffraction grating. Some useful discussion about fabrication process is also provided to improve the top-layer etching diffraction grating in tri-layer Si_3N_4 waveguides.

2. Design of top-layer etching diffraction grating

The proposed waveguide diffraction grating on tri-layer Si_3N_4 waveguide is shown in Fig. 1.[14] There are three Si_3N_4 layers on the substrate of silicon. There are SiO_2 layers between three Si_3N_4 layers and on the substrate. The upper cladding is also SiO_2 layer. The top Si_3N_4 layer is etched as the diffracting layer. The other two Si_3N_4 layers and SiO_2 layer works as a guiding waveguide and reflecting layer. The

†Corresponding author. E-mail: liujingwei@cspctech.com
‡Corresponding author. E-mail: zshan@ime.ac.cn

© 2025 Chinese Physical Society and IOP Publishing Ltd. All rights, including for text and data mining, AI training, and similar technologies, are reserved.

diffraction angle of the grating in air medium is determined by

$$\sin\theta = n_{\mathrm{g}} - \frac{\lambda_0}{\Lambda}, \tag{1}$$

where Λ is the period, $n_{\mathrm{g}} = (1-d_{\mathrm{c}})n_{\mathrm{etch}} + d_{\mathrm{c}}n_{\mathrm{unetch}}$ is the effective index of the waveguide grating, d_{c} is the duty cycle, n_{unetch} and n_{etch} are the effective indices of the non-etched and etched waveguides, respectively.

In order to enhance the upward efficiency at a specific diffraction angle, the grating efficiency can be controlled by tuning the etched layer thickness t_3 and the duty cycle d_{c}. The grating period Λ should be adjusted accordingly due to the variation in the effective index [Eq. (1)].The core structure (the first Si_3N_4 (t_1), SiO_2 layers (g_1), and the second Si_3N_4 layer (t_2)) can be seen as a one-dimensional (1D) photonic crystal (1DPC) and will be optimized using the photonic band-gap theory to minimize the reflection. An optimal design at 905 nm in Table 1 is developed using finite-difference time-domain (FDTD) algorithm, which shows a diffraction efficiency of 91.6% and a far-field divergence angle of 0.103°.

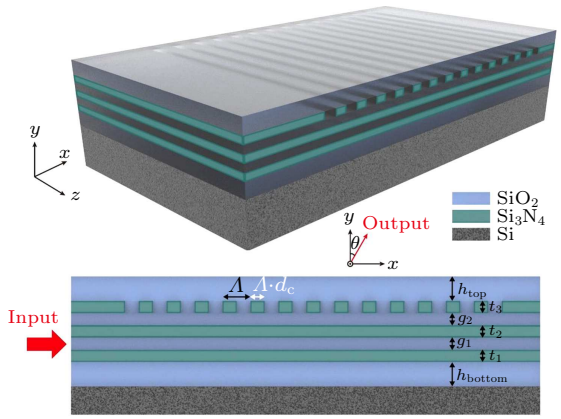


Fig. 1. The proposed diffraction grating with the only etched top-layer in tri-layer Si_3N_4 optical waveguides: (a) three-dimensional (3D) view of the grating structure and (b) cross-sectional view in the x–y plane.

A test chip is designed to evaluate the waveguide diffraction grating on tri-layer Si_3N_4 as shown in Fig. 2. The testing sample of the diffraction grating consists of three parts, which are a diffraction grating for light output from waveguides, a coupling grating for light input into waveguide, and a waveguide beam expander, respectively. Among them, two types of grating have different etching depths. The flat diffraction grating only was etched in top-layer of tri-layer silicon nitride waveguides. On the other side, the coupling grating was etched in the full three layers of silicon nitride waveguides. Between them, the waveguide beam expander was designed for tuning and matching the widths of different grating waveguides. And, the cross-sectional structure is shown in Figs. 2(b) and 2(c).

The optical path principle shown is as follows: the light beam from an external laser is incident on the coupling grating by the optical fiber, the coupling grating converts the off-chip beam into the TE_{00} transmission mode of the on-chip waveguide, the TE_{00} mode in the waveguide is adiabatic gradually transformed to the fundamental mode distribution of the waveguide with the width of 100 μm through the beam expander, and then diffracted to the off-chip through the flat diffraction grating. The total loss of the optical path of the test structure includes the optical fiber coupling loss, the waveguide transmission loss, the beam expander loss and the flat diffraction grating diffraction loss. The input coupling grating and waveguide beam expander has the coupling loss and the waveguide transmission loss, so as to extract the diffraction loss of the flat diffraction grating from the overall loss.

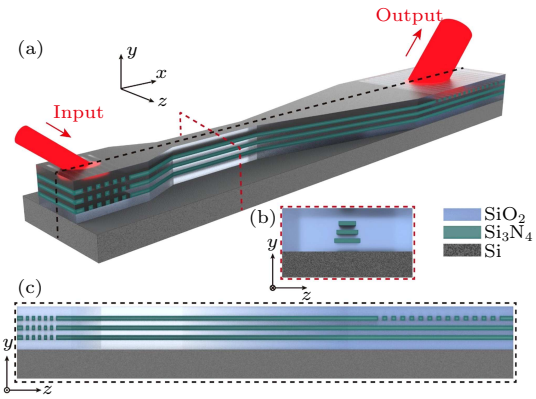


Fig. 2. The test chip consists of a proposed output diffraction grating, an input coupling grating, and a waveguide beam expander: (a) isometric view, (b) y–z view, (c) y–x view.

3. Preparation process steps

The preparation process steps and chip structure of the test chip are shown in Fig. 3, including the following four steps:

(i) Substrate preparation: An optical chip is decomposed from an 8-inch (1 inch = 2.54 cm) substrate wafer. The substrate wafer was made by its preparation process as follows: the silicon wafer is thermally oxidized to grow a silicon oxide lower cladding, and then the LPCVD method is used to deposit lower, middle, and then upper layer silicon nitride and upper/lower layer silicon oxide.

(ii) Lithography and etching of tri-layer silicon nitride fully etched waveguide: A uniformly positive photoresist is applied to the substrate, and the area of the pattern to be etched is exposed by an electron beam, with the critical size of no less than 200 nm. After the photoresist is developed, the reactive ion etching (RIE) method is used to alternately etch the silicon nitride and silicon oxide layers, forming a fully etched strip waveguide.

(iii) Lithography and etching of top-layer silicon nitride shallow etched waveguide: Based on fully etched waveguide chips, uniform positive photoresist is used, and lithography is

used to expose the shallow etched pattern area. After development, RIE method is also used to etch the upper layer silicon nitride, forming a flat diffraction grating waveguides.

(iv) Finally, deposition of silicon oxide cladding: PECVD method is used to deposit the silicon oxide cladding, with the thickness of about several microns.

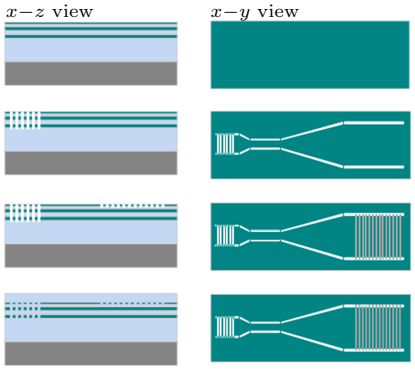


Fig. 3. Preparation process steps and chip structure schematic diagram of diffraction gratings testing structure.

4. Chip characterization

The structural parameters of measurement and design for the tri-layer Si_3N_4 waveguide diffraction grating are summarized in Table 1. There is no measured data for the thickness of the lower cladding and core layer, and the actual parameters are determined by the preparation accuracy of the substrate. Based on the empirical data provided by the manufacturer, the thickness deviation of each layer is within ±5%.

Table 1. The structural parameters of tri-layer Si_3N_4 waveguide diffraction gratings at 905 nm.

Structures	Units	Design	Measurement	Difference
Λ	μm	0.495	0.488	–0.007
d_c	/	0.5	0.44	–0.06
h_{top}	μm	1.40	1.399	–0.001
t_3	μm	0.053	–	–
g_2	μm	0.132	–	–
t_2	μm	0.114	–	–
g_1	μm	0.157	–	–
t_1	μm	0.114	–	–
h_{bottom}	μm	3.300	–	–

Before and after depositing the silicon oxide coating (process step (iv)), the cross-sectional structure of the prepared chip was observed and measured using a focused ion beam-dual beam electron microscope, as shown in Fig. 4. Before depositing the cladding (Fig. 4(a)), if the measured etching depth of the process test pattern is 80.5 nm, the upper layer of silicon oxide was etched exactly, stop at the bottom of the etched top-layer, and the upper layer of silicon nitride is a little over etched, matching the design requirements. The actual measured width of the pattern with a design width of 294 nm is 179.4 nm, and the pattern deviation is −114.6 nm. Therefore, the deviation between the actual tooth width of the diffraction grating with a tooth width compensation of +85 nm and the design value is 229.6 nm; The measured grating period is 488.4 nm, with a deviation of −6.6 nm from the design value of 495 nm, and duty cycle d_c of the etching region is set as 0.5, with a deviation of about −0.06, as shown in Table 1. After depositing the cladding (Fig. 4(b)), an air gap structure can be seen between adjacent grating teeth in the cladding.[18,19] The red color in the figure represents the silicon nitride layer in a single cycle of the grating test pattern.

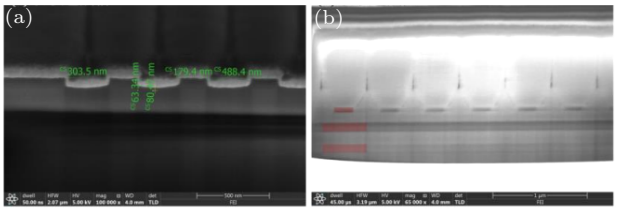


Fig. 4. The SEM images of the chip process monitoring: (a) process monitoring image without cladding, (b) process monitoring image with oxide clads by PECVD.

5. Results and discussion

5.1. Measurement results of proposed diffraction gratings

The test sample is fabricated with a total of four flat diffraction gratings in each set as shown in Fig. 5. One can observe that the outgoing beam from the diffraction zone of the diffraction grating clearly observed from the microscope.



Fig. 5. Observation photo of flat diffraction grating microscope.

Based on the truncation method, the insertion losses (*IL*) of each group were tested, which is composed of reflection loss (*RL*), coupling loss (*CL*), and diffraction loss (*DL*) as shown in Table 2. The diffraction loss (*DL*) test values of four sets of flat diffraction grating waveguide samples (Nos. 1–4) are within the range of 0.23 dB to 0.59 dB, with an average value of 0.44 dB. The difference between the overall loss of the diffraction path and the coupling loss of the fiber, resulting in a deviation in *DL*.

Table 2. The loss and upward diffraction efficiency of diffraction gratings in tri-layer Si_3N_4 optical waveguides.

	Unit	1#	2#	3#	4#	AVE
IL	dB	12.46	12.22	12.28	12.44	12.35
RL	dB	0.77	0.88	0.95	0.60	0.80
CL	dB	11.22	11.11	11.04	11.39	11.19
$DL = IL - RL - CL$	dB	0.47	0.23	0.59	0.45	0.44
$\eta = 10^{-DL/10}$	/	0.897	0.948	0.873	0.902	0.905

The corresponding average upward diffraction efficiency ($\eta = 10^{-DL/10}$) is 90.5%, which is in good agreement with

the design value of 91.6%. It should be noted that the upward diffraction efficiency of the grating sample No. 2 is higher than the theoretical value, which may be mainly due to the testing error introduced by the consistency of fiber coupling loss.

5.2. The far-field divergence angle of proposed diffraction gratings

Four sets of diffraction gratings in tri-layer optical Si_3N_4 waveguides were tested for their far-field intensity distribution as shown in Fig. 6. Among them, figure 6(a) shows the grayscale image captured by an infrared camera, and figure 6(b) shows the average grayscale in the red box selection area in Fig. 6(a). Distribution of directions and extraction is based on the far-field divergence angle of θ. The full width of $1/e^2$ of the directional distribution is used as the far-field divergence angle.

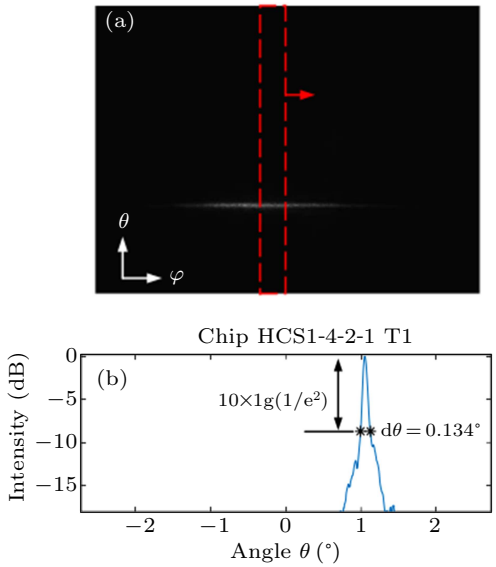


Fig. 6. Far field diffraction intensity distribution of a diffraction grating: (a) infrared cameras capture images, (b) the average grayscale edge of red box selected area image.

The testing results of the far-field divergence angle for four grating samples are summarized in Table 3. The average value of directional measurement is 0.154°, which is larger than the theoretical value of 0.103°.

Table 3. Far-field divergence angle of diffraction gratings for 4 samples.

Far field divergence angle	Unit	1#	2#	3#	4#	AVE
$d\theta$	degree	0.138	0.145	0.161	0.173	0.154

The deviation between the measured and theoretical values of far-field divergence angle is from the difference of fabricated samples and designed configures for the diffraction grating. In fact, there is an air gap in the adjacent grating tooth cladding (as shown in Fig. 5(b)), which deviates from an ideal design of grating waveguides. Therefore, parasitic extraction and post-layout simulation was conducted on the grating unit containing the air gap. However, the calculation results showed that air gaps did not change the near-field effective length of the grating in percentage, which did not cause changes in the far-field divergence angle either.

As the theoretical model, the diffraction angle of the grating is significantly correlated with the grating period. Near the grating period of 495 nm, the rate of change of the diffraction angle with the grating period is 0.217 °/nm. Therefore, the diffraction structures of grating waveguides are really sensitive to the process of lithography and development. In the case of random fluctuations in the 0.2 nm grating period caused by rounding errors or positioning deviations, it is possible to widen the far-field divergence angle of the grating by 0.05°. Therefore, in order to achieve a smaller far-field divergence angle, the machining accuracy of the grating cycle needs to be further improved, or the design value of the grating divergence angle needs to be further reduced to leave machining deviation redundancy.

6. Conclusion

An experimental diffraction grating with the only etched top-layer in tri-layer Si_3N_4 waveguides is demonstrated. The design and preparation process steps are provided for the diffraction grating. Four testing sample of the diffraction grating are fabricated, which consists of a diffraction grating for light output from waveguides, a coupling grating for light input into waveguide, and a waveguide beam expander. The measurement results of the diffraction grating with only etched top-layer in tri-layer Si_3N_4 waveguides at a wavelength of 905 nm show the average upward diffraction efficiency of 90.5%, which shows a good agreement with the design value of 91.6%, and average far-field divergence angle of 0.154°, which is larger than the design value of 0.103°. The big difference of far-field divergence angle between the design and the experiment is the random deviation of the grating period in the preparation of grating diffraction structures. In order to obtain a smaller far-field divergence angle, the preparation deviation of the grating period must be controlled less than 0.2 nm.

Acknowledgements

Project supported by the National Key Research and Development Program of China (Grant No. 2022YFB2802401) and the Beijing Municipal Natural Science Foundation (Grant No. Z221100006722002).

References

[1] Buzaverov K A, Baburin A S, Sergeev E V, *et al.* 2024 *Laser Photon. Rev.* **18** 2400508
[2] Blasco-Solvas M, Fernández-Vior B, Sabek J, *et al.* 2024 *J. Lightwave Technol.* **42** 6019
[3] Buzaverov K A, Baburin A S, Sergeev E V, *et al.* 2023 *Opt. Express* **31** 16227

[4] Hong J X, Spring A M, Qiu F, *et al*. 2019 *Sci. Rep.* **9** 12988
[5] Subramanian A Z, Selvaraja S, Verheyen P, *et al*. 2012 *IEEE Photon. Technol. Lett.* **24** 1700
[6] Daldosso N, Melchiorri M, Riboli F, *et al*. 2004 *J. Lightwave Technol.* **22** 1734
[7] Zou J H, Yu Y, Ye M Y, *et al*. 2015 *Opt. Express* **23** 26305
[8] Zhang H J, Li C, Tu X G, *et al*. 2014 *Opt. Express* **22** 21800
[9] Doerr C R, Chen L, Chen Y, *et al*. 2010 *IEEE Photon. Technol. Lett.* **22** 1461
[10] Zhang H J, Li C, Tu X G, *et al*. 2014 *Appl. Phys. A* **115** 79
[11] Asaduzzaman M, Bakaul M, Skafidas E, *et al*. 2018 *Sci. Rep.* **8** 2540
[12] Laere F V, Roelkens G, Ayre M, *et al*. 2007 *J. Lightwave Technol.* **25** 151
[13] Taillaert D, Laere F V, Ayre M, *et al*. 2006 *Jpn. J. Appl. Phys.* **45** 6071
[14] Li W L, Liu J W, Cheng G A, *et al*. 2022 *Appl. Opt.* **61** 2604
[15] Raval M, Poulton C V and Watts M R 2017 in *Conference on Lasers and Electro-Optics, OSA Technical Digest (online), paper STh1M.5*
[16] Chen B S, Li Y Z, Zhang L X, *et al*. 2021 *Opt. Express* **29** 20995
[17] Roeloffzen C G H, Hoekman M, Klein E J, *et al*. 2018 *IEEE J. Sel. Top. Quantum Electron.* **24** 1
[18] Tyler N A, Fowler D, Malhouitre S, *et al*. 2019 *Opt. Express* **27** 5851
[19] Li W L, Liu J W, Cheng G A, *et al.* 2023 *IEEE Photon. J.* **15** 6600207